4D label-free quantitative proteomic and phosphoproteomic profiling of the kidney in rat models of antimyeloperoxidase-associated vasculitis

C. Zhao[1,2], H. Xiong[2], Z. Zheng[3], L. Zhang[4], C. Bian[2], M. Zhao[2], Y. Li[2], J. Li[2]

[1]School of Medicine, Henan University of Chinese Medicine, Henan; [2]Department of Forensic Medicine, Chongqing Medical University, Chongqing; [3]College of Basic Medicine and Forensic Medicine, Henan University of Science and Technology, Henan; [4]School of Basic Medical Sciences, Chongqing College of Traditional Chinese Medicine, Chongqing, China.

Abstract

Objective

The early diagnosis of antimyeloperoxidase (anti-MPO) -associated vasculitis is still a challenge in clinical practice. This study aimed to facilitate the early diagnosis of anti-MPO-associated vasculitis and investigate its pathogenesis.

Methods

We established an animal model of experimental autoimmune vasculitis (EAV), and applied 4D label-free technology to identify proteins and phosphorylated proteins in the kidneys of the EAV group and control group.

Results

A total of 674 differentially expressed proteins (DEPs) were identified by proteomics, including 347 up-regulated and 327 down-regulated proteins. The results of the GO and KEGG enrichment analysis showed that DEPs were mainly involved in complement and coagulation cascade reactions, as well as the formation of neutrophil extracellular traps. According to the analysis of MCODE and hub proteins, FGG, HRG, C3, SERPIND1, ITIH2, A2M were selected as target proteins, and parallel reaction monitoring (PRM) was used to validate the above proteins. The validation results were consistent with the proteomic detection results. Through de-background analysis of differentially expressed phosphorylated proteins, a total of 497 differentially expressed phosphorylated attributed proteins were identified, 256 of which were down-regulated and 241 were up-regulated. These proteins mainly participated in energy metabolism-related pathways. The prediction analysis of upstream phosphorylated kinases suggested that kinases with significantly up-regulated activity included CAMK2D, PAK2, CAMK2B, and PRKAA2, while kinases with down-regulated activity included ADRBK1 and PLK1.

Conclusion

The results of this study could provide some auxiliary indicators for the early diagnosis of anti-MPO-associated vasculitis, and provide a basis for further understanding of its pathogenesis.

Key words

anti-MPO-associated vasculitis, kidney, proteomic, phosphoproteomic

Congcong Zhao, MD
Hongli Xiong
Zhe Zheng, MD
Li Zhang, MD
Cunhao Bian
Minzhu Zhao, MD
Yongguo Li
Jianbo Li, MD, Prof.

Please address correspondence to:
Jianbo Li
Department of Forensic Medicine, Chongqing Medical University, Chongqing 400010, China.
E-mail: 100390@cqmu.edu.cn

Received on July 30, 2024; accepted in revised form on November 18, 2024.

Funding: the research was funded by the Distinguished Professor Program of Chongqing Medical University (R1025).

Competing interests: none declared.

Introduction

Systemic vasculitis (SV) is an autoimmune disease characterised primarily by vascular wall necrosis and inflammatory cell infiltration. SV can affect various blood vessels and organs, such as the kidneys, lungs, and brain, resulting in diverse clinical manifestations, which can be life-threatening in severe cases (1-3). Currently, the diagnosis of SV usually relies on histopathological examination, however, if clinicians and forensic workers encounter situations such as a lack of medical records or atypical microscopic manifestations, it often leads to missed diagnosis or misdiagnosis.

According to the size of the diseased blood vessels, vasculitis is divided into large-, medium- and small-vessel vasculitis. Among them, small-vessel vasculitis includes anti-neutrophil cytoplasmic antibody (ANCA)-associated vasculitis and immune complex associated vasculitis. ANCA mainly includes myeloperoxidase (MPO)-ANCA and protease 3 (PR3)-ANCA. In epidemiological investigations of SV in Asian countries, myeloperoxidase (MPO) is a relatively important target antigen, but the pathogenesis of anti-MPO-associated vasculitis remains unclear (4-6). In recent years, with the rapid development of molecular biology technology, label-free proteomics has entered the 4D era. A fourth dimension (ionic mobility) was added based on the dimensionality division of mass/charge ratio (m/z), retention time, and ion strength, which improved the accuracy and richness of quantification (7, 8). In this study, differentially expressed proteins (DEPs) in renal tissues of experimental autoimmune vasculitis (EAV) rats were screened by 4D label-free proteomics and phosphoproteomic technology. Bioinformatics analysis of the data was performed to identify hub proteins and mechanisms involved in anti-MPO-associated vasculitis. The DEPs were further validated through parallel reaction monitoring (PRM). These findings will enable us to further reveal the pathogenesis of anti-MPO-associated vasculitis at the molecular level and may provide potential targets for its early clinical diagnosis and treatment.

Materials and methods

Animals treatment and sample collection

Twenty male Sprague-Dawley rats (Specific Pathogen Free, 200-250 g) were purchased from the Animal Experimental Center of Chongqing Medical University. All the animals were raised in a Specific Pathogen Free (SPF) standard animal laboratory. Twenty rats were randomly divided into EAV group and control group: the rats in the EAV group were subcutaneously injected with recombinant MPO-CFA emulsifier (0.14 mg/100 g) on the first day, and recombinant MPO-IFA emulsifier (0.7 mg/100 g) on day 7; the control group was immunised by BSA. All rats in the EAV group and control group were intravenously injected with a low dose of sheep anti-rat GBM serum on days 28 and 29 (9). On the next day (day 30), the rats were placed in metabolic cages to collect urine, and after centrifugation, the supernatant was taken and stored at -80°C. On the 32nd day, all rats were anaesthetised with pentobarbital (4%, 1 mL/100 g) and sacrificed by cervical dislocation, then the heart blood and kidneys were collected for further study.

Humoral immune responses to MPO

ELISA was used to detect plasm anti-MPO IgG titres, plasm was either added directly or serially diluted, Detected by horseradish peroxidase conjugated sheep anti-rat IgG.

Assessment of renal injury

Urine albuminuria was detected by ELISA and expressed as ng/24 hrs. The formalin-fixed kidney samples (n=6, 3 in each group) were sliced into 4 μm paraffin sections, then stained with haematoxylin and eosin (HE) to observe the histopathological features.

Protein extraction and digestion

The kidney samples were ground at low temperature, then lysed using a buffer (0.2% SDS, 8M urea, 100 mM ammonium bicarbonate, pH=8), and the supernatant was obtained after centrifugation. 10 mM DTT was added to the supernatant, mixed and placed at

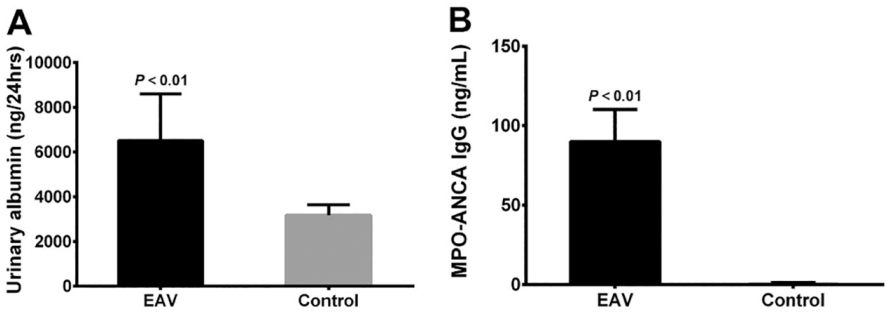

Fig. 1. The contents of 24-hour urinary albumin and plasma MPO-ANCA IgG in EAV and control group. **A**: the content of 24-hour urinary albumin; **B**: the levels of plasma MPO-ANCA IgG.

56°C for 1 h. A sufficient amount of IAM was added, and the samples were left standing at room temperature for 1 h away from light. Cooled acetone was added to the samples, and placed at -20°C for 2 h, the precipitation was collected after low temperature centrifugation. Protein solution (6M urea, 100 mM TEAB, pH=8.5) was added to the sample to dissolve the precipitation. The quality of proteins was checked by Bradford method and SDS-PAGE. Finally, to the protein samples were added trypsin, DB protein solution (8 M urea, 100 mM TEAB, pH=8.5), and 100 mM TEAB buffer, and let stand at 37°C for 4 hours. Then add $CaCl_2$ and trypsin were added to initiate overnight digestion at 37°C. The resulting peptides were desalted with C18 column, washed repeatedly with cleaning solution 3 times, The eluted peptides were freeze-dried under vacuum. For the phosphoproteome, peptide mixtures were enriched for phosphorylated peptides using IMAC-Fe column (10, 11).

Ultra high-performance liquid chromatography phase (uhplc) fractionation and lc-ms/ms analysis

Total peptide and phosphopeptide-enriched samples were dissolved in buffer A (100% water, 0.1% formic acid) respectively, after centrifuged, the supernatants were obtained and loaded onto EASY-nLC™ 1200nanoElute upgrades UHPLC systems. Peptides were separated by buffer B (80% acetonitrile, 0.1% formic acid) with different gradient concentration.The separated peptides were analysed by tandem mass spectrometry on the Q Exactive™ HF-X mass spectrometer, with a full-scan MS (350 to 1500 m/z). The parent ions with the TOP 30 ionic strength in the full-scan were splintered by high energy collision induced dissociation (HCD), and secondary mass spectrometry was performed.

The following device parameters were used: full-scan resolution, 120000 (200m/z); secondary mass spectrometry resolution, 15000 (200 m/z); dynamic exclusion duration, 20 s.

Protein identification and bioinformatic analysis

Maxquant 2.0.3.0 was used to analyse the mass spectrometer data. According to the fold change (FC) of proteins, DEPs and differentially phosphorylated proteins were screened. Proteins with FC >1.5 and a *p*-value <0.05 were considered up-regulated, while proteins with FC <1/1.5 and a *p*-value <0.05 were considered down-regulated (12). The online DAVID software (https://david-d.ncifcrf.gov/) was used for the Gene Ontology (GO) analysis of DEPs. After annotation, Kyoto Encyclopedia of Genes and Genomes (KEGG) pathways (http://www.genome.jp/kegg/) was used for the pathway enrichment analysis. The Interproscan software was used for the enrichment of functional domains of DEPs. The DEPs were imported into the STRING database to create a protein-protein interaction network, then the analysis results were imported into Cytoscape 3.7.1 for data visualisation. MCODE was used to cluster the DEPs, and the degree algorithm of CytoHubba was used to screen the Hub genes.

Proteomics combined with phosphoproteomic

The differentially phosphorylated attributed protein was obtained by de-background analysis of differentially phosphorylated proteins. Kinase pre-

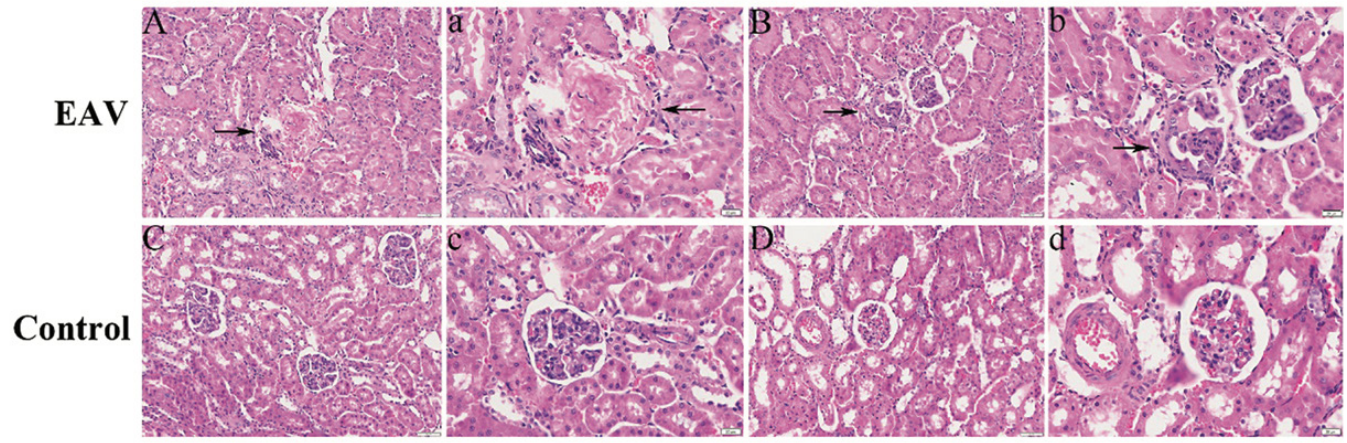

Fig. 2. Histopathological observation of renal tissue in EAV group and control group.
(**A, a, B, b**) EAV group; (**C, c, D, d**) control group. (**A, a**) glomerular fibrosis. (**B, b**) cellular crescent formation. (**A, B, C, D**) 100×; (**a, b, c, d**) 200×.

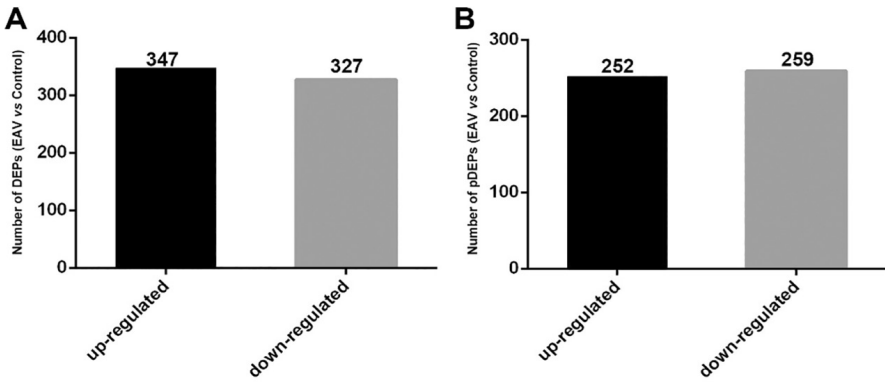

Fig. 3. Distribution levels of differentially expressed or phosphorylated proteins in the EAV group compared with the control group.
A: The number of proteins whose expression levels were significantly up-regulated or down-regulated in the EAV group compared with the control group;
B: The number of phosphorylated proteins whose expression levels were significantly up-regulated or down-regulated in the EAV group compared with the control group.

diction was performed by the NetworkIN algorithm to screen out kinases with high scores, and the kinase activity was analysed by Kinase-Substrate Enrichment Analysis (KSEA).

Parallel reaction monitoring

To further verify the DEPs, six selected proteins were quantified by PRM. The methods of protein extraction and trypsin digestion were the same as the 4D label-free experiment. The peptide samples were detected by QExactive HF mass spectrometer combined with UltiMate 3000 RSLCnano liquid phase. The data obtained were retrieved by Maxquant 2.0.3.0 software and then

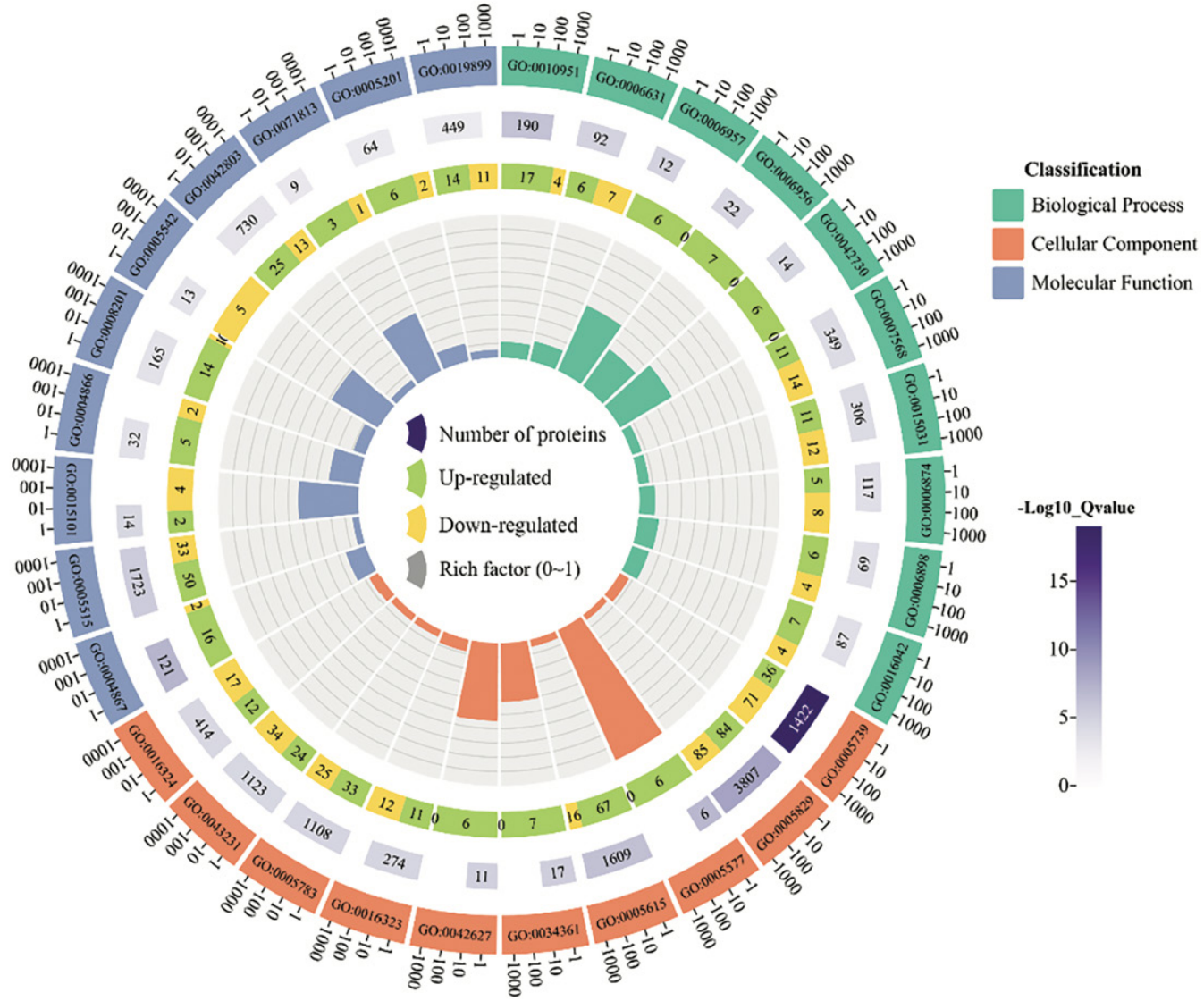

Fig. 4. GO analysis of 674 DEPs in EAV group vs Control group. The terms of biological process, cell component and molecular function were indicated in green, orange and purple respectively. The number of DEPs, up-regulated proteins and down-regulated proteins contained in each category was labelled.

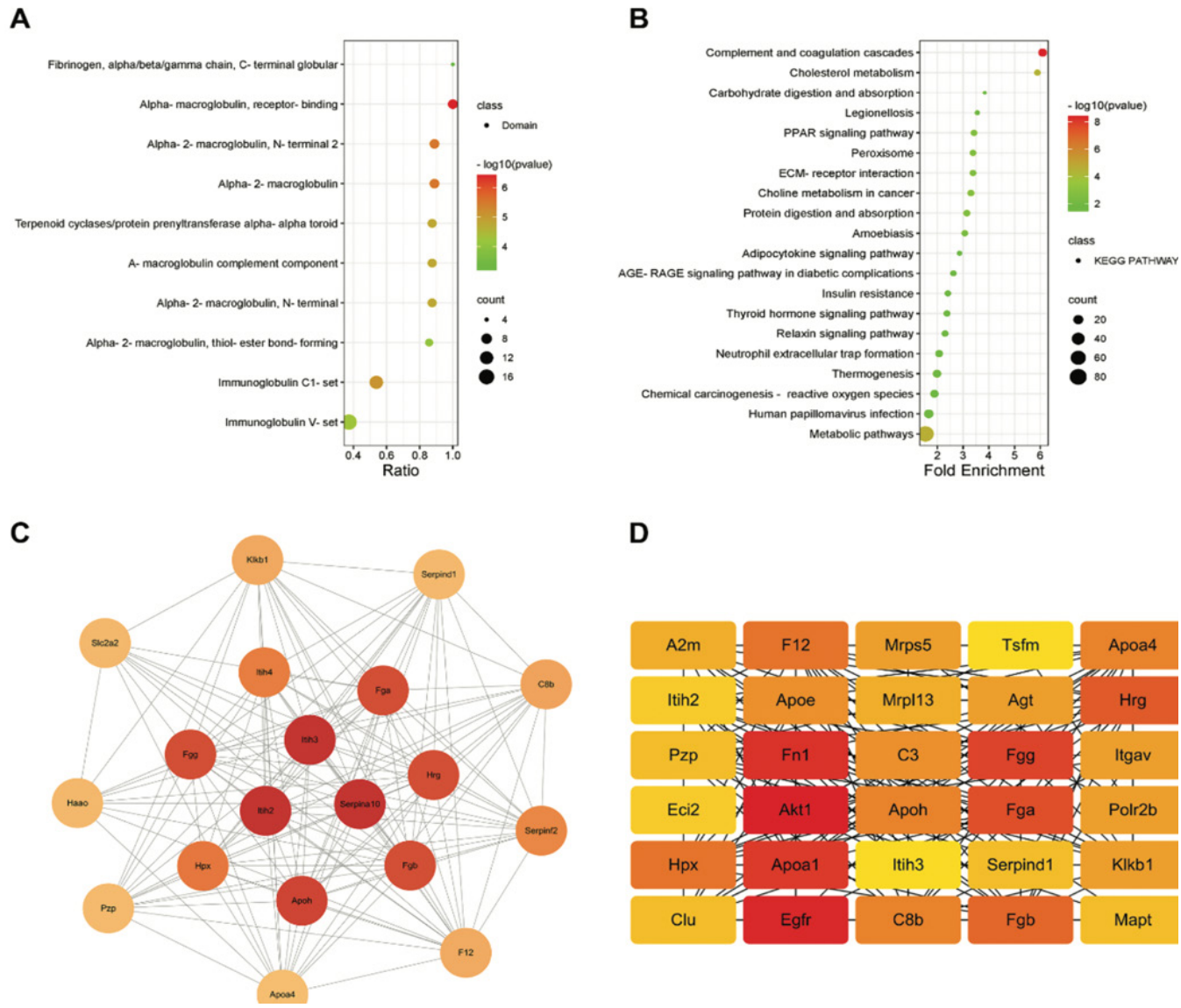

Fig. 5. Analysis of domains, KEGG pathways and interactions of differentially expressed proteins.
A: the top 10 domains with the lowest *p*-value; **B**: the top 20 KEGG pathways with the lowest *p*-value; **C**: the key MCODE module; (**D**) PPI network of the top 30 hub proteins.

imported into Skyline software for quantitative analysis of proteins.

Ethics approval

All animal procedures for this study were performed in accordance with the Guide for the Care and Use of Laboratory Animals and approved by the Animal Care and Use Committee of Chong Qing Medical University (Acceptance no.: IACUC-CQMU-2023-12023).

Statistics

The quantitative data were compared between the two groups by student's t-test, a *p*-value <0.05 was considered statistically significant.

Results

The contents of 24-hour urinary albumin and plasm MPO-ANCA IgG

The 24-hour urine of rats in the experimental group (EAV group) and control group was collected on the next day (day 30) after the injection of a low dose of sheep anti-rat GBM serum, and albumin was detected (Fig. 1A). The results showed that the 24-hour urinary albumin level in the EAV group (6509 ±738.5 ng) was significantly higher than the control group (3175±191.1 ng), and the difference was statistically significant ($p<0.01$). Plasma of the experimental group and the control group were collected and MPO-ANCA IgG was detected (Fig. 1B). Compared with the control group (0.4880±0.3087 ng/mL), the EAV group (89.96±6.409 ng/mL) was significantly higher than the EAV group (0.4880±0.3087 ng/mL), and the difference was statistically significant ($p<0.01$).

Histopathological observation of the kidney

HE staining was performed on the kidneys of the two groups of rats, and the results showed that the rats in the EAV group had glomerular fibrosis (as shown by arrows in Fig. 2A and Fig. 2a), and some glomeruli showed cellular crescent formation and base-

ment membrane thickened (as shown by arrows in Fig. 2B and Fig. 2b). In the control group, the glomerular was normal and no obvious pathological changes were observed.

Identification of differentially expressed proteins

Three kidney samples from each group were randomly selected for 4D label-free proteomic analysis to identify the differentially expressed proteins (DEPs). A total of 29868 unique peptides corresponding to 4188 proteins were identified in this study. Proteins with FC >1.5 (or <0.67) and $p<0.05$ were considered as DEPs. Based on the above screening criteria, 674 DEPs were differentially expressed, of which 347 DEPs were up-regulated and 327 DEPs were down-regulated (Fig. 3A). Phosphoproteomic results showed that 3273 phosphorylated proteins were identified and 511 phosphorylated differentially expressed proteins (pDEPs) were screened, 252 of which were up-regulated and 259 were down-regulated (Fig. 3B).

The functional annotation and enrichment analysis of the differentially expressed proteins

The biological processes, cellular components, and molecular functions of 674 DEPs were obtained by GO annotation analysis. With $p<0.05$ as the screening criterion, the top 10 GO annotation results with the smallest p-value were selected and their data are visualised in Figure 4. The biological processes associated with these DEPs included negative regulation of endopeptidase activity, fatty acid metabolic process, complement activation, alternative pathway, complement activation, fibrinolysis. The cellular components enriched mainly included mitochondria, cytosol, fibrinogen complex, extracellular space, very-low-density lipoprotein particle. The molecular function involved included serine-type endopeptidase inhibitor activity, protein binding, organic cation transmembrane transporter activity, endopeptidase inhibitor activity and heparin binding.

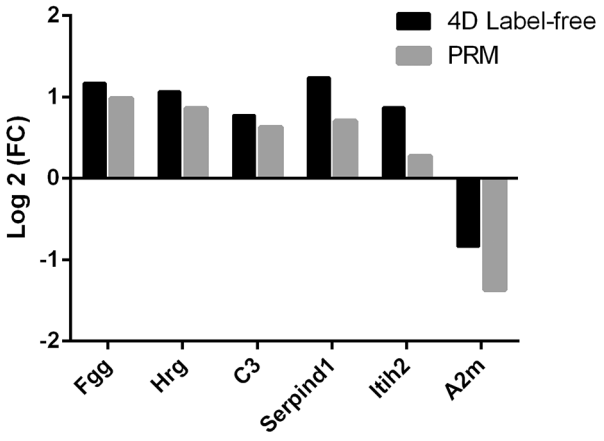

Fig. 6. Comparison of 4D label-free and PRM quantitative results of renal DEPs in EAV group *vs*. Control group.

Analysis of differentially expressed proteins for enrichment in domains and KEGG pathways, protein-protein interactions and modules

DEPs were enriched in the following domains (Fig. 5A): fibrinogen α/β/γ chain -C terminal globular domain, α-macroglobulin receptor binding, α2-macroglobulin (n-terminal 2), α2-macroglobulin, terpenoid cyclase/protein isopentenyltransferase (α-α ring), A-macroglobulin complement component, α2-macroglobulin (n-terminal), α-2- Macroglobulin (thiol ester bond formation), immunoglobulin C1 group, immunoglobulin V-set. The results of the KEGG pathway (Fig. 5B) showed that the main enrichment pathways of DEPs included complement and coagulation cascade, metabolic pathway, human papillomavirus infection, thermogenesis, chemical carcinogenic-reactive oxygen species, and neutrophil extracellular trap formation.

We predicted interactions between DEPs using STRING and Cytoscape, and the protein-protein interaction network revealed the key module (Fig. 5C), with MCODE score = 16.11. The module contained 19 DEPs, 16 of which were up-regulated and 3 were down-regulated. The pathways involved included complement and coagulation cascade (Fgb, Fga, Serpind1, F12, Serpind2, Fgg, C8b, Klkb1), coronator-COVID-19 (Fgb, Fga, Fgg, C8b), platelet activation (Fgb, Fga, FGA, C8B, Fgg), neutrophil extracellular trap formation (Fgb, Fga, Fgg), and all the DEPs contained in the above pathways were up-regulated. The top 30 DEPs (with high scores) were identified by degree classification method in CytoHubba (Fig. 5D). Combined with the analysis results of MCODE modules, 6 proteins were identified as hub proteins: Fgg, Hrg, C3, serind1, Itih2 and A2m. These proteins were verified by PRM analysis, and the results indicated that the expression levels of Fgg, Hrg, C3, serind1 and Itih2 in EAV group were up-regulated, while A2m levels were down-regulated, which were consistent with the results of proteomic (Fig. 6).

De-background analysis of differentially phosphorylated protein

A total of 674 DEPs were screened by proteomics, and 511 pDEPs were identified by phosphoproteomic. Through the de-background analysis of pDEPs, 14 proteins were found to have the same expression trend with phosphorylated proteins, and 497 differentially expressed phosphorylated attributed proteins were obtained, among which 241 proteins were up-regulated and 256 proteins were up-regulated.

The functional annotation and enrichment analysis of the differentially expresses phosphorylated attributed proteins

GO analysis of differentially expressed phosphorylated attributed proteins showed that the enriched biological processes included glutathione metabolism, cell response to cAMP, microtubule cytoskeleton structure, tricarboxylic acid cycle, and selenium ion response. The cell components included cytoplasm, cell fluid, mitochondria, nucleus and perinuclear region of

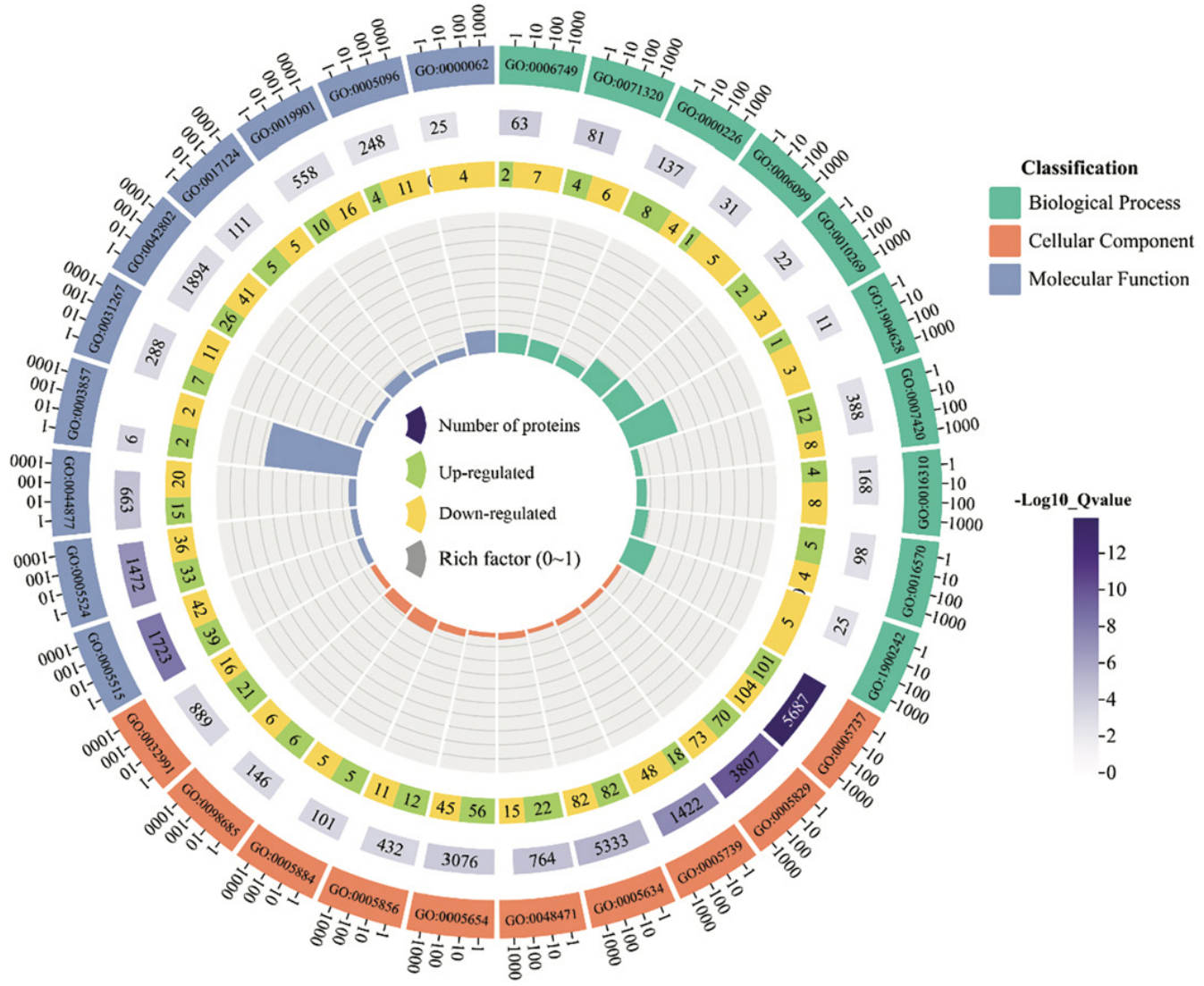

Fig. 7. GO analysis of 497 differentially expressed phosphorylated attributed proteins in EAV group *vs*. Control group. The terms of biological process, cell component and molecular function were indicated in green, orange and purple respectively. The number of proteins, up-regulated proteins and down-regulated proteins contained in each category was labelled.

cytoplasm. In addition, the molecular functions include protein binding, ATP binding, macromolecular complex binding, 3-hydroxyl-CoA dehydrogenase activity, and small GTPase binding (Fig. 7).

Analysis of differentially expresses phosphorylated attributed proteins for enrichment in domains and KEGG pathways, protein-protein interactions and modules

We used Interproscan software to conduct domain annotation analysis on the differentially expresses phosphorylated attributed proteins. With $p<0.05$ as the standard, 10 domains with the lowest p-value were selected (Fig. 8A). The enriched domains included: acetaldehyde dehydrogenase domains; aldehyde dehydrogenase, C-terminal; aldehyde/histamine dehydrogenase; aldehyde dehydrogenase, N-terminal; pleckstrin homologous domain, etc. The enriched KEGG pathways included carbon metabolism, citric acid cycle (TCA cycle); metabolic pathway; amyotrophic lateral sclerosis; thermogenesis; degradation of valine, leucine and isoleucine. (Fig. 8B).

The protein-protein interaction network of differentially expresses phosphorylated attributed proteins was analysed by the MCODE plug-in of Cytoscape software. Two critical modules were identified as shown in Figures 8C and 8D. MCODE 1 (MCODE Score = 6.452) contained 32 proteins, of which 10 proteins are up-regulated and 22 proteins are down-regulated, and the pathways involved included ribosome and coronavirus disease-novel coronavirus pneumonia. MCODE 2 (MCODE Score = 4.571) contained 22 proteins, 7 of which 7 were up-regulated and 15 down-regulated. The KEGG pathway analysis showed that the proteins were mainly involved in metabolism, thermogenesis, and citric acid cycle (TCA cycle). The top 30 DEPs (with high scores) identified by degree classification method in CytoHubba are shown in Figure 8E, including Actb, Crebbb, Sdha, Atp5a1, Atp5b.

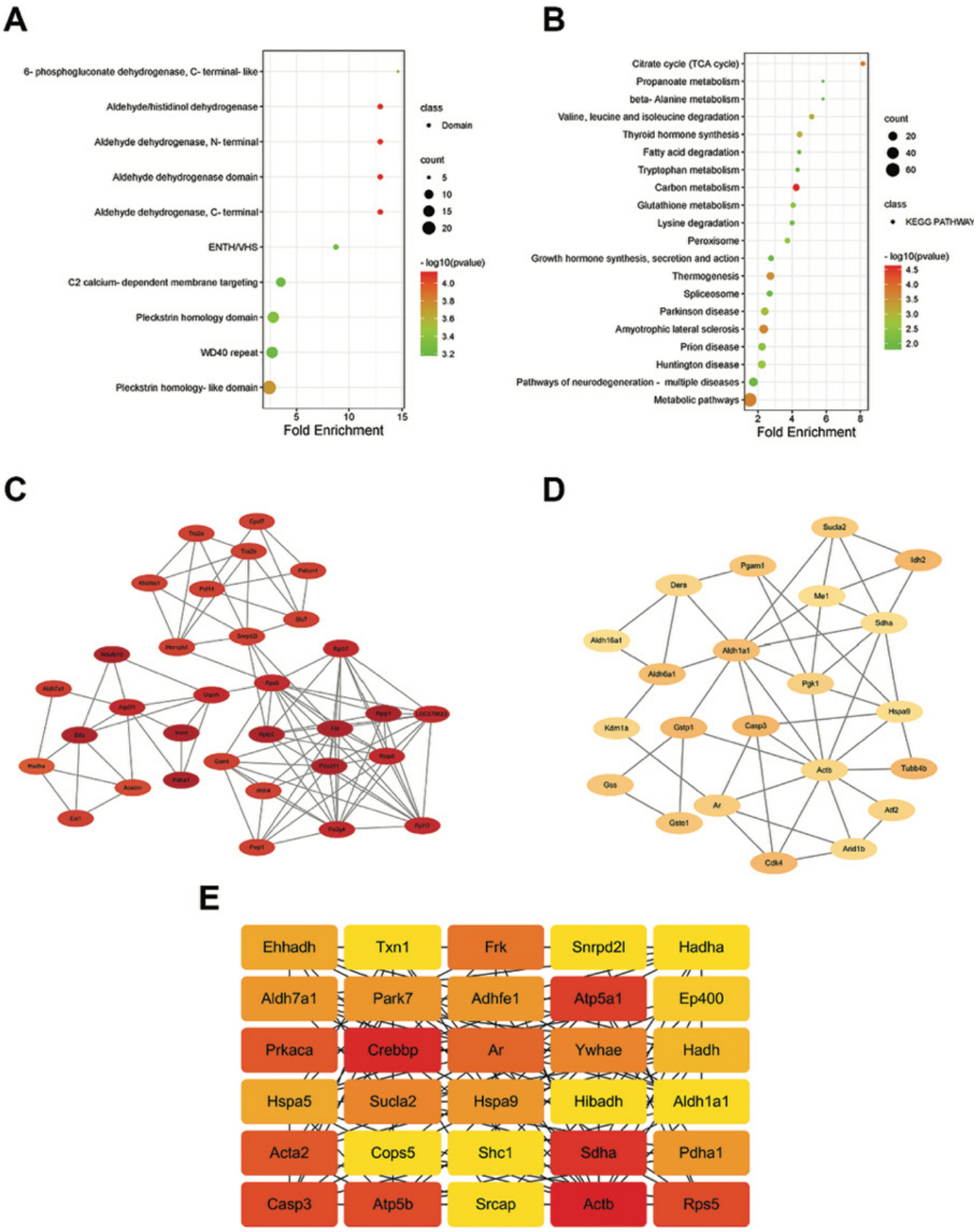

Fig. 8. Analysis of domains, KEGG pathways and interactions of differentially expresses phosphorylated attributed proteins.
A: the top 10 domains with the lowest *p*-value; **B**: the top 20 KEGG pathways with the lowest *p*-value; **C**: MCODE 1; **D**: MCODE 2; **E**: PPI network of the top 30 hub proteins.

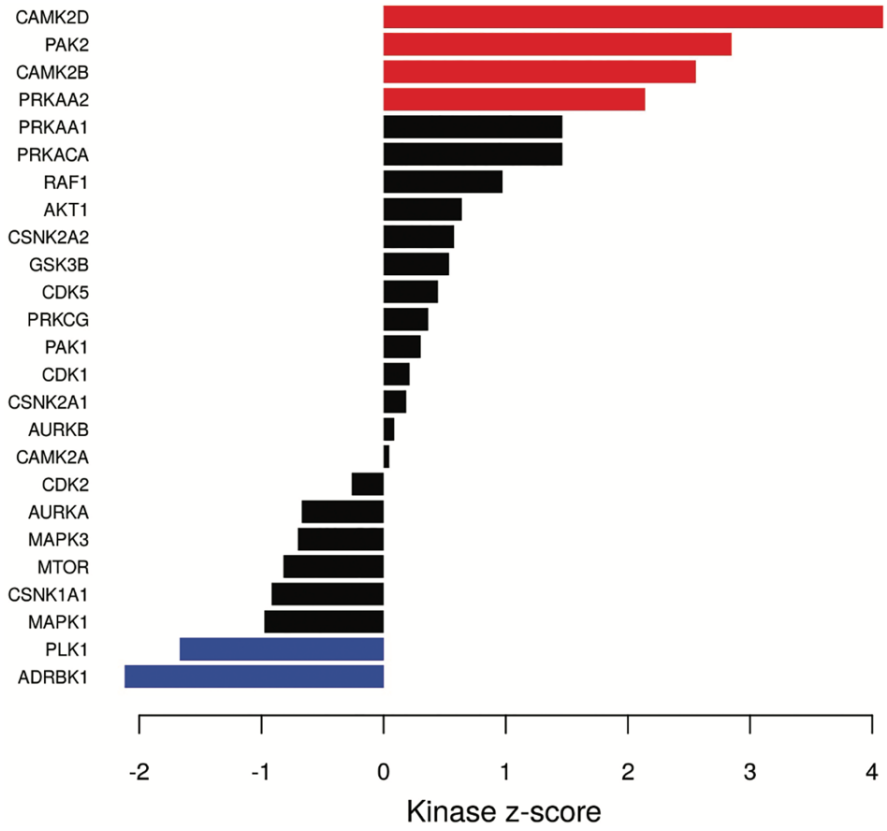

Fig. 9. The result of kinase activity analysis.
Red represents kinases with upregulated activity and blue represents kinases with significantly down-regulated activity.

Motif analysis of the phosphosites

The modified amino acids identified in the EAV and the control group included serine (S), threonine (T) and tyrosine (Y), and most of them were serine. After motif analysis of phosphorylated modification sites, NetworkIN algorithby degree classification method in CytoHubba are shown in Figure 8E, including Actb, Crebbb, Sdha, Atp5a1, Atp5b.

Motif analysis of the phosphosites

The modified amino acids identified in the EAV and the control group included serine (S), threonine (T) and tyrosine (Y), and most of them were serine. After motif analysis of phosphorylated modification sites, the NetworkIN algorithm was used to predict upstream kinases, and 84 phosphorylated network groups were obtained. KSEA analysis was performed to predict the activity of kinase, as shown in Figure 9 (with Z-score > 0 indicating up-regulated activity and Z-score < 0 indicating down-regulated activity). The results showed that the kinases with significantly up-regulated activity included CAMK2D, PAK2, CAMK2B and PRKAA, and the kinases with significantly down-regulated activity included ADRBK1 and PLK1.

Discussion

At present, gross morphology and microscopic observation of organs or tissues are still commonly used in clinical or forensic pathological diagnosis of anti-MPO-associated vasculitis. However, in the early stage of anti-MPO-associated vasculitis, histopathological changes are not obvious, which is easy to cause diagnosis difficulties, and it is urgent to find molecular markers with high sensitivity and specificity to assist in the diagnosis of anti-MPO-associated vasculitis. So far, some scholars have conducted proteomic studies on Kawasaki disease, Behçet's disease, giant cell arteritis, etc. However, the above studies were limited to structural proteomics and did not involve functional proteomics (13-15). In this study, by combining proteomics with phosphoproteomic, biological information can be mined from the two perspectives of protein abundance and modification level, providing new ideas for the diagnosis, treatment and pathogenesis of anti-MPO-associated vasculitis.

In this study, the results of proteomics showed that compared with the control group, DEPs mainly focused on the negative regulation of endopeptidase activity, complement activation, fibrinolysis, cellular calcium ion homeostasis, etc., suggesting that renal DEPs in EAV played a role in regulation of endopeptidase activity and immune function. The KEGG pathway enrichment results showed that DEPs were significantly enriched in complement and coagulation cascade. Abnormal activation of the complement system can promote the production of inflammatory cytokines and chemokines as well as recruitment of immune cells, leading to tissue damage, pathological inflammation and activation of coagulation pathway. Previous studies have shown that this signalling pathway is involved in the pathogenesis and clinical manifestations of various autoimmune diseases such as systemic lupus erythematosus and vasculitis (16, 17). In addition, the pathway enrichment results showed that 13 DEPs were involved in the formation of neutrophil extracellular traps, which is believed to play an important role in the pathogenesis of haematological diseases and is closely related to anti-MPO-associated vasculitis (18, 19). We also validated 6 hub proteins by PRM, and the results were consistent with proteomics.

FGG, HRG, C3 and SERPIND1 are involved in the coagulation process and immune regulation (20-23). Our results showed that these proteins were up-regulated in the EAV group, confirming that the hypercoagulable state of blood was closely related to the susceptibility of anti-MPO-associated vasculitis to thrombosis. In addition, the activation of neutrophils and the generation of inflammatory reactions also aggravated vascular injury. Interalpha trypsin inhibitor Heavy chain 2 (ITIH2) is one of the components of interalpha trypsin inhibitor (ITI). ITI interact with extracellular matrix molecules and play a key role in maintaining homeostasis in various tis-

sues (24). Several studies have found that increased expression of ITI family proteins is associated with a variety of pathological conditions, including tissue injury, tissue repair, and inflammation (25, 26). Jiang *et al*. (27) found that the expression of ITIH2 was increased in urine of patients with systemic lupus erythematosus (SLE) associated with kidney injury. In our study, the expression level of ITIH2 was significantly up-regulated, indicating the presence of kidney injury in the EAV group.

α2-macroglobulin (A2M) is a broad-spectrum protease inhibitor, which is involved in anti-oxidation, anti-fibrosis, anti-inflammation, homeostasis and other processes. In addition, Becker *et al*. (28) found the position of A2M on the surface of the blood vessel wall, and this protease inhibitor could protect the vascular endothelium from potentially damaging intravascular protease. In this study, A2M was significantly down-regulated in the EAV group, indicating that its inflammation was aggravated, and its vascular protective effect was decreased, leading to vascular injury.

Through the combined analysis of proteomics and phosphoproteomics, GO and KEGG enrichment results suggest that differentially phosphorylated attributed proteins participate in metabolism related pathways in mitochondria and cytoplasm, which is consistent with previous studies that have found abnormal energy metabolism to play an important role in autoimmune diseases and inflammatory responses (29, 30). In addition, thermogenesis is also an important pathway enriched in our study, and thermogenesis is significantly associated with increased body temperature, which is one of the common symptoms of anti-MPO-associated vasculitis. The activity of upstream phosphorylated kinases was further predicted, and the results showed that the kinases with significantly up-regulated activity included CAMK2D, PAK2, CAMK2B, PRKAA, etc., while the kinases with significantly down-regulated activity included ADRBK1, PLK1, etc. Among them, CAMK II as an intracellular calcium signal receptor, has been proved to be expressed in endothelial cells, vascular smooth muscle cells and monocytes, and its abnormal activation is closely related to vascular injury (31, 32).

In conclusion, the expression of renal DEPs in EAV group confirmed that complement and coagulation cascade and neutrophil extracellular trap pathway play an important role in its pathogenesis. Meanwhile, hub proteins were screened and verified by PRM method. It was confirmed that some proteins such as FGG, HRG, C3, SERPIND1, ITIH2 and A2M were important for the study of anti-MPO-associated vasculitis. In addition, through the combined analysis of proteomics and phosphoproteomics, we found that differentially phosphorylated belonging proteins affect the occurrence and development of anti-MPO-associated vasculitis by participating in energy metabolism-related pathways. The up-regulation activity of CAMK II kinase plays an important role in vascular injury. It is expected that these proteins and kinases will be further studied for the early diagnosis of anti-MPO-associated vasculitis and provide new ideas for its treatment.

At present, the animal model of EAV is an important tool for studying anti-MPO-associated vasculitis. Through continuous improvement and perfection of the animal model of EAV, it can be closer to the pathological characteristics and clinical manifestations of human anti-MPO-associated vasculitis, which will help to improve the reliability and translation of the research results. Therefore, the results of this study can provide some valuable information for the research and treatment of human anti-MPO-associated vasculitis, such as the study of pathogenesis, diagnostic markers, immunotherapy and so on. In addition, adequate clinical trials and validation are required when translating the results of animal experiments into clinical applications.

References

1. TREPPO E, MONTI S, DELVINO P *et al*.: Systemic vasculitis: one year in review 2024. *Clin Exp Rheumatol* 2024; 42(4): 771-81. https://doi.org/10.55563/clinexprheumatol/gkve60
2. SHARMA P, SHARMA S, BALTARO R, HURLEY J: Systemic vasculitis. *Am Fam Physician* 2011; 83(5): 556-65.
3. BASU N, KARABAYAS M, PUSEY C: Prognosis and future developments in vasculitis. *Best Pract Res Clin Rheumatol* 2018; 32 (1): 148-65. https://doi.org/10.1016/j.berh.2018.08.011
4. BERTI A, CORNEC D, CROWSON CS, SPECKS U, MATTESON EL: The epidemiology of antineutrophil cytoplasmic autoantibody-associated vasculitis in Olmsted County, Minnesota: a twenty-year US population-based study. *Arthritis Rheumatol* 2017; 69(12): 2338-50. https://doi.org/10.1002/art.40313
5. PEARCE FA, CRAVEN A, MERKEL PA, LUQMANI RA, WATTS RA: Global ethnic and geographic differences in the clinical presentations of anti-neutrophil cytoplasm antibody-associated vasculitis. *Rheumatology* (Oxford) 2017; 56(11): 1962-69. https://doi.org/10.1093/rheumatology/kex293
6. MOHAMMAD AJ: An update on the epidemiology of ANCA-associated vasculitis. *Rheumatology* (Oxford) 2020; 59 (Suppl 3): iii42-iii50. https://doi.org/10.1093/rheumatology/keaa089
7. LOGINOV DS, FIALA J, CHMELIK J, BRECHLIN P, KRUPPA G, NOVAK P: Benefits of ion mobility separation and parallel accumulation-serial fragmentation technology on timsTOF pro for the needs of fast photochemical oxidation of protein analysis. *ACS Omega* 2021; 6(15): 10352-61. https://doi.org/10.1021/acsomega.1c00732
8. BHATTACHARYYA IM, COHEN S, SHALABNY A, BASHOUTI M, AKABAYOV B, SHALEV G: Specific and label-free immunosensing of protein-protein interactions with silicon-based immunoFETs. *Biosens Bioelectron* 2019; 132: 143-61. https://doi.org/10.1016/j.bios.2019.03.003
9. GAN PY, DICK J, O'SULLIVAN KM *et al*.: Anti-CD20 mAb-induced B cell apoptosis generates T cell regulation of experimental myeloperoxidase ANCA-associated vasculitis. *J Am Soc Nephrol* 2021; 32(5): 1071-83. https://doi.org/10.1681/asn.2020060834
10. WU J, AN Y, PU H *et al*.: Enrichment of serum low-molecular-weight proteins using C18 absorbent under urea/dithiothreitol denatured environment. *Anal Biochem* 2010; 398(1): 34-44. https://doi.org/10.1016/j.ab.2009.10.047
11. WU J, XIE X, LIU Y *et al*.: Identification and confirmation of differentially expressed fucosylated glycoproteins in the serum of ovarian cancer patients using a lectin array and LC-MS/MS. *J Proteome Res* 2012; 11(9): 4541-52. https://doi.org/10.1021/pr300330z
12. LIN H, ZHANG W, XU Y *et al*.: 4D label-free quantitative proteomics analysis to screen potential drug targets of Jiangu Granules treatment for postmenopausal osteoporotic rats. *Front Pharmacol* 2022; 13: 1052922. https://doi.org/10.3389/fphar.2022.1052922
13. CHAUDHARY H, NAMEIRAKPAM J, KUMRAH R *et al*.: Biomarkers for Kawasaki disease: clinical utility and the challenges ahead. *Front Pediatr* 2019; 7: 242 https://doi.org/10.3389/fped.2019.00242
14. HU CJ, PAN JB, SONG G *et al*.: Identification of novel biomarkers for Behcet disease diagnosis using human proteome microarray approach. *Mol Cell Proteomics* 2017; 16(2): 147-56. https://doi.org/10.1074/mcp.m116.061002

15. RÉGENT A, LY KH, GROH M *et al*.: Molecular analysis of vascular smooth muscle cells from patients with giant cell arteritis: Targeting endothelin-1 receptor to control proliferation. *Autoimmun Rev* 2017; 16(4): 398-406. https://doi.org/10.1016/j.autrev.2017.02.006
16. LEFFLER J, BENGTSSON AA, BLOM AM: The complement system in systemic lupus erythematosus: an update. *Ann Rheum Dis* 2014; 73(9): 1601-6. https://doi.org/10.1136/annrheumdis-2014-205287
17. TRIVIOLI G, VAGLIO A: The rise of complement in ANCA-associated vasculitis: from marginal player to target of modern therapy. *Clin Exp Immunol* 2020; 202(3): 403-6. https://doi.org/10.1111/cei.13515
18. PAPAYANNOPOULOS V: Neutrophil extracellular traps in immunity and disease. *Nat Rev Immunol* 2018; 18(2): 134-47. https://doi.org/10.1038/nri.2017.105
19. RADA B: Neutrophil extracellular traps. *Methods Mol Biol* 2019; 1982: 517-28. https://doi.org/10.1007/978-1-4939-9424-3_31
20. MANCO L, SILVA C, FIDALGO T, MARTINHO P, SARMENTO AB, RIBEIRO ML: Venous thromboembolism risk associated with ABO, F11 and FGG loci. *Blood Coagul Fibrinolysis* 2018; 29(6): 528-32. https://doi.org/10.1097/mbc.0000000000000753
21. WAKE H: Histidine-rich glycoprotein modulates the blood-vascular system in septic condition. *Acta Med Okayama* 2019; 73(5): 379-82. https://doi.org/10.18926/amo/57366
22. GEISBRECHT BV, LAMBRIS JD, GROS P: Complement component C3: A structural perspective and potential therapeutic implications. *Semin Immunol* 2022; 59: 101627. https://doi.org/10.1016/j.smim.2022.101627
23. HOFFMAN M, PRATT CW, BROWN RL, CHURCH FC: Heparin cofactor II-proteinase reaction products exhibit neutrophil chemoattractant activity. *Blood* 1989; 73(6): 1682-85.
24. LORD MS, MELROSE J, DAY AJ, WHITELOCK JM: The inter-α-trypsin inhibitor family: versatile molecules in biology and pathology. *J Histochem Cytochem* 2020; 68(12): 907-27. https://doi.org/10.1369/0022155420940067
25. KIM B, DE LA MONTE S, HOVANESIAN V *et al*.: Ontogeny of inter-alpha inhibitor protein (IAIP) expression in human brain. *J Neurosci Res* 2020; 98(5): 869-87. https://doi.org/10.1002/jnr.24565
26. HENNIES HC: All is balanced: inter-α-trypsin inhibitors as unseen extracellular matrix proteins in epidermal morphology and differentiation. *Exp Dermatol* 2015; 24(9): 661-62. https://doi.org/10.1111/exd.12771
27. JIANG J, ZHAO J, WANG Y, LIU D, ZHANG M: Urine inter-alpha-trypsin inhibitor family-related proteins may serve as biomarkers for disease activity of lupus. *J Clin Lab Anal* 2022; 36(9): e24622. https://doi.org/10.1002/jcla.24622
28. BECKER CG, HARPEL PC: alpha2-Macroglobulin on human vascular endothelium. *J Exp Med* 1976; 144(1): 1-9. https://doi.org/10.1084/jem.144.1.1
29. XU Y, CHEN Y, ZHANG X *et al*.: Glycolysis in innate immune cells contributes to autoimmunity. *Front Immunol* 2022; 13: 920029. https://doi.org/10.3389/fimmu.2022.920029
30. CHEN J, LIU C, YE S, LU R, ZHU H, XU J: UPLC-MS/MS-based plasma lipidomics reveal a distinctive signature in systemic lupus erythematosus patients. *MedComm (2020)* 2021; 2(2): 269-78. https://doi.org/10.1002/mco2.67
31. EBENEBE OV, HEATHER A, ERICKSON JR: CaMKII in Vascular Signalling: "Friend or Foe"? *Heart Lung Circ* 2018; 27(5): 560-67. https://doi.org/10.1016/j.hlc.2017.12.003
32. TOUSSAINT F, CHARBEL C, ALLEN BG, LEDOUX J: Vascular CaMKII: heart and brain in your arteries. *Am J Physiol Cell Physiol* 2016; 311(3): C462-C478. https://doi.org/10.1152/ajpcell.00341.2015